A Three-Tiered Approach to Assessing Changes in Fire Danger in the Northern Rockies under Different Climate Change Projections

Anthony DiBiase[1]
Duke University, Durham, NC, 27708

Andrew Kumler[2]
University of Illinois, Urbana, IL, 61801

Matthew Lammers[3]
University of Utah, Salt Lake City, UT, 84112

and

Rama Nemani[4]
NASA Ames Research Center, Moffett Field, CA, 94035

Nomenclature

CMIP5	Coupled Model Intercomparison Project Version 5
CFFDRS	Canadian Forest Fire Danger Rating System
TOPS	Terrestrial Observation and Prediction System
WRF	Weather Research and Forecasting
BNU-ESM	Beijing National University Earth System Model
CanESM2	Canadian Earth System Model Version 2
CSIRO-Mk3.6.0	Commonwealth Scientific and Industrial Research Organization Mark 3.6.0
GFDL-ESM2G	Geophysical Fluid Dynamics Laboratory Earth System Model Version 2, GOLD Ocean
GFDL-ESM2M	Geophysical Fluid Dynamics Laboratory Earth System Model Version 2, Modular Ocean
MIROC5	Model for Interdisciplinary Research On Climate Version 5
MRI-CGCM3	Meteorological Research Institute Coupled Global Climate Model Version 3

Abstract

This project looks at three methods assessing the impacts projected climate change could have on wildland fire danger and behavior in the Greater Glacier National Park region. At 800-meter resolution, Drought Code, a component of CFFDRS was calculated for daily output of multiple models within CMIP5. Using TOPS, modifications to fuel loading and gross primary productivity were assessed. Finally, in locations found to be most susceptible to increased fire danger, we ran the WRF model with the SFIRE extension to compare shifts in fire spread regime based on atmospheric projections and anticipated shifts in vegetation type. Our study found that monthly mean values of Drought Code for the summer months are anticipated to increase under most climate projections, and critically high values of Drought Code are anticipated to spread into regions currently believed to be

[1]Master's Student, Nicholas School of the Environment, Duke University
[2]Master's Student, Department of Atmospheric Science, University of Illinois, Urbana-Champaign
[3]Master's Student, Department of Atmospheric Science, University of Utah
[4]Senior Earth Scientist, Ecological Forecasting Laboratory, NASA Ames Research Center

less susceptible to fire. Modeled runs generated from WRF-FIRE demonstrate significantly greater wildfire impacts compared to a baseline current scenario.

I. Introduction

a. Ecological Modeling

The ability to model ecosystems to better understand the processes involved is of great use to scientists and decision-makers. Integrating climate model and satellite data, along with various ecological constants, helps interested parties evaluate the historical and future health of a particular ecosystem or protected area. The Terrestrial Observation and Prediction System (TOPS) is an ecological model used by research scientists at NASA Ames Research Center to study protected areas, such as Yosemite National Park, among others[1]. With this model, we plan to investigate the Greater Glacier National Park area for its changes in Gross Primary Production (GPP), Vapor Pressure Deficit (VPD), and soil moisture. These three variables have been proven to be key indicators of ecosystem health and wildfire ignition[2,3].

Climate change will have drastic and varying effects on protected areas such as Glacier National Park, so it is of interest to the NPS and its rangers/managers to better understand how various ecosystems change in their respective park. These changes can alter how wildfires will spread and initiate in the future, which can severely alter the appearance of the park, and its ecosystem dynamics. With TOPS, we hope to provide some insight into these changes.

b. Drought Modeling

The 2012 wildfire season in the Western United States demonstrated how diverse the impacts are of fire on the livelihoods of those residing or vacationing in the region. Hundreds of homes were destroyed in Colorado in two separate conflagrations. Smoke pollution plagued towns and cities in Washington, Idaho, and Utah, in some cases from fires hundreds of miles away. Officials closed highways and national forests vital for recreation due to fire and smoke danger. While initially 2012 might appear to be a statistical outlier, already this year, we have seen further devastation in Colorado, as well as the deaths of 19 volunteer firefighters in Arizona. While small-scale atmospheric factors such as dry thunderstorms and downslope windstorms play a key role in fire ignition and spread, we cannot dismiss the role of humans, "who are changing landscapes to be more or less flammable, as well as lighting and extinguishing fires."[4]

This study explores the first half of the above quote: the impact of anthropogenic climate change on making landscapes more or less susceptible to wildfire. With the explosion of global climate model (GCM) development intertwined with unceasing increases in computing power, the scientific community's understanding of the specific impacts of climate change has grown over the last decade. The recent Coupled Model Intercomparison Project 5 (CMIP5) created a framework for current-generation models to be run in a manner such that their outputs could easily be distributed to scientists and then compared[5]. Previous climate model analyses studying susceptibility of landscapes to wildfire based on atmospheric variables focused on two methodologies. Scientists developed statistical models to correlate historical fire danger/occurrence and then projected that model into the future[6-10]. Other studies calculated currently used fire indices under future conditions to determine anticipated anomalies from climatological values[11-13].

It is the latter approach that we used for this study, investigating specifically Drought Code as calculated as part of the Canadian Forest Fire Danger Rating System (CFFDRS) [14]. The CFFDRS suite of indices was used in Flannigan and Van Wagner, as well as Tymstra, et al. We focused specifically on the RCP 4.5 radiative projection, viewed as the "medium mitigation scenario,"[15] and the geographic region surrounding Glacier National Park. Our initial hypothesis was that Drought Code, being driven entirely by temperature and precipitation, would increase in lower-elevation regions based on climate projections of temperature. Mid-elevation slopes and valleys would also show increases in Drought Code values, with values typically seen in the low-elevation regions pushing higher in elevation. High-elevation regions would remain less clear due to uncertainty as to precipitation distributions and consistently low temperatures. Regardless, fire in higher elevations in Glacier is unlikely due to the lack of fuels above treeline.

c. *Fire Behavior Modeling*

Global climate change presents a major challenge to land managers seeking to protect ecosystem functionality and human welfare in the face of increasingly larger wildfires[6]. While many regions in the Western United States exhibit a historical fire regime exemplified by small surface brushfires essential to carbon cycling, plant regeneration, and numerous other ecological processes, rising temperatures and a higher frequency of drought

are predicted to significantly change fire behavior, especially in the context of nearly a century of fire suppression and fuel buildup[6,16,17]. These projected changes in fire behavior in high-risk regions demand an improved approach to modeling fire spread. The complexity and multi-dimensional scale of wildfires across a landscape make precise numerical approximation virtually impossible: even with powerful parallel supercomputing capacity, many current "workhorse" fire models necessitate simplification of important weather and atmospheric variables. Current widely accepted software programs for understanding fire behavior, notably FARSITE[18] and BehavePlus[19], operate by projecting a two-dimensional fire model on a spatial grid, using Roethermal's[20] semi-empirical fire spread equations and a pre-set global wind direction. While suitable for rough estimates of fire spread in a faster than real-time operational environment (such as during a wildfire, or a prescribed burn), the lack of complex weather in these models requires an inevitable reduction in their ability to simulate realistic fire-weather feedback[21].

We attempt to overcome the computational limitations to projecting wildfire behavior under conditions of climate change by using a next-generation, three-dimensional and multi-scalar fire model, the SFIRE extension to the Weather Research and Forecasting (WRF)[22-24]. By coupling an advanced mesoscale weather prediction model to Roethermal's[20] spread equations, SFIRE is capable of anticipating highly local fire-weather feedback; wind plays a role in fire spread, which conversely affects atmospheric processes. Wildfires often generate distortions in local atmospheric conditions by heating air and increasing the velocity of low-level winds, which have a profound influence on fire spread and behavior. Given projected changes in regional climate over the next century, it is essential to understand wildfire behavior jointly with weather processes. SFIRE thus enables significantly more sophisticated analysis of the role wildfires will play in ecosystems under conditions of global climate change[21].

WRF/SFIRE is built primarily as an experimental model rather than an operational software program, and is designed for research purposes rather than faster than real-time analysis. Validation by Kochanski et al.[25] and others[26,27] have yielded relatively high-accuracy results using fine-resolution topographic and fire fuel data. The model is limited, however, to depicting the spread of surface ground fires rather than crown fire movement and spotting. Given the fire regime in our selected study area is prone to occasional large-scale stand-replacing fire events, which are predicted to occur in higher frequency with climate change, this limitation presents a significant barrier. Despite this limitation, the coupled atmospheric-fire model at the core of WRF/SFIRE presents a powerful three-dimensional tool for visualizing and simulating fire spread according to cell-by-cell weather-fire feedback.

To assess the viability of WRF with the SFIRE extension as a suitable tool for regional-scale fire behavior modeling, we ran it in a roughly 100km^2 region encompassing Glacier National Park, in the Northern Rockies region of the United States. An analysis of existing literature indicates that past efforts involving WRF with SFIRE have been limited to a narrow geographic resolution, which is significantly smaller than the scale required for land management decision support toolkits[26,27]. We anticipate WRF/SFIRE will scale successfully to larger regional analysis. Our research provides a framework for the usage of WRF/SFIRE for simulation of wildfire events at a regional, allowing resource managers to anticipate the influence of future changed weather conditions on fire regimes across an entire ecological landscape.

II. Methods

The region of focus in this analysis is a roughly 223.09 km. by 152.15 km. rectangle encompassing Glacier National Park and the surrounding region in Western Montana (Fig. 1). The ecology varies widely by elevation, ranging from high-alpine to coniferous forest dominated by *Pseudotsuga menziesii*, *Picea engelmannii*, and *Pinus albicaulis*, to wide rangelands at the lower elevations. The elevation gradient extends from 1000-3000 meters, with precipitation ranging from 50-120 cm. annually[28]. Dendrochonological analysis via tree fire-scar dating reveals a history of small surface brushfires at a 25-75 year interval, with stand-replacing crown fires at a mean 200-year interval[17]. High resolution, landscape-level topographical data was obtained from the United States Geological Survey's "National Map" database at a 1/3-Arc Second resolution for the study region. Further existing ground fuel data was obtained at a 1-Arc Second resolution from the Forest Service and USGS jointly WRF weather models, was obtained from NCAR via the online WRF User Support Page. Data were converted to a geoTiff file and merged to form a single file for the full domain using the GDAL geoprocessing library in Python. Weather data was obtained for a six hour time period during July 1, 2013 from North American Regional Reanalysis (NARR) dataset, a product of the National Oceanic and Atmospheric Organization (NOAA).

a. Ecological Modeling

Our goal for this study is to investigate how wildfire regimes will change into the 21st century in the Greater Glacier National Park area, given certain parameters. We chose this area because it appears many studies that involve Glacier National Park are those focused on the glaciers themselves, while studies on the ecology and resultant wildfire patterns of this area are less abundant.

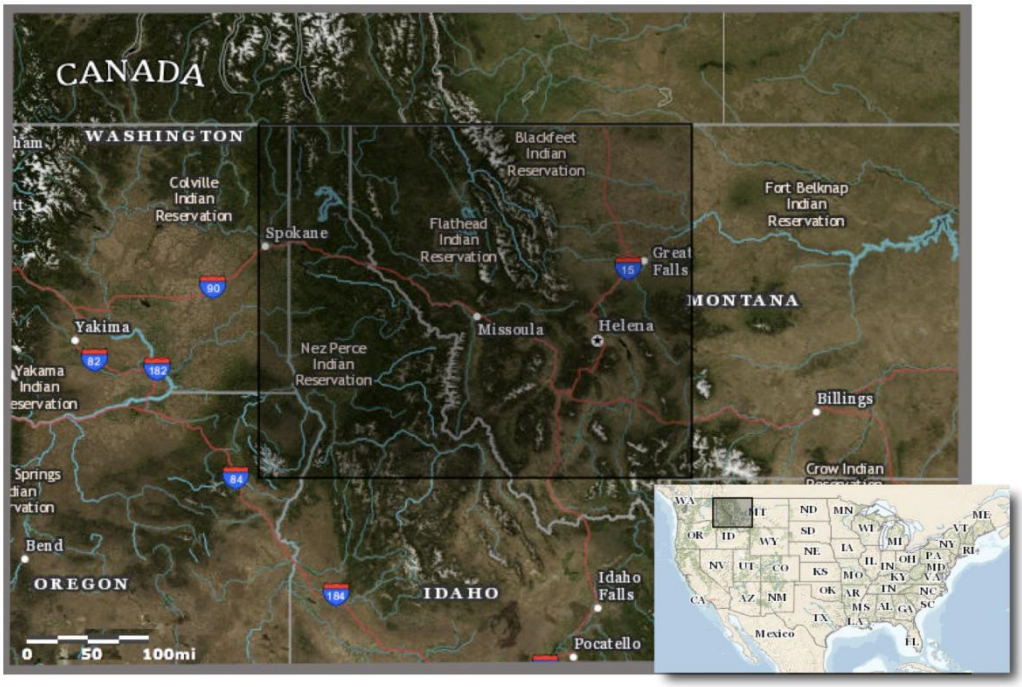

Figure 1. Primary study area and selected domain. *The region of focus is bounded by the darker rectangle in the map, ending at the northern boundary of the United States. The region contains parts of Washington and Idaho, but is primarily located in Montana (illustrated by the included subset map as well). Map data adapted from Landsat imagery and USGS 7.5-minute Topo available from the USGS National Map database.*

From the ecological modeling perspective of this investigation, we ran TOPS with a 1 km^2 grid cell size, which stretched a half-degree of latitude and a full degree longitude. The result was a domain of 14,884 grid cells modeled over the entire Greater Glacier National Park area. This 122 km^2 area consists of highly varying terrain and ecosystems, which can play a vital role in how wildfire will spread within the park[29].

After picking a domain, we chose the time scales on which our study would operate. Three periods were chosen: one historical (1970-1999), one near-term (2006-2035), and one long-term (2066-2095), all of which are 30-year intervals. We thought it important that in order to look at the near future and further out, a historical run towards the end of the 20th century would be a helpful base case. Prior to the historical run, a 10-year spin up of TOPS was performed in order to obtain reasonable values for GPP and soil moisture[30].

Inputs into TOPS are wide-ranging, including: climate model data, satellite-based data, ground-based weather measurements, and other ecological constants. For the climate data, we used downscaled CMIP5 data that was available via NEX (NASA Earth Exchange), which inputs monthly maximum temperature, minimum temperature, VPD, solar radiation, and precipitation values at the 800-meter scale. Vast arrays of CMIP5 variables are available, but for the purposes of this study, were not relevant[31]. Of the different climate scenarios available, we chose RCP 4.5 (Representative Concentration Pathway), which is a scenario that aims to stabilize radiative forcing at 4.5 W/m^2 in the year 2100[32]. Another part of this scenario is how CO_2 will stabilize into the 21st century. For the three time periods mentioned above, discrete values were chosen accordingly. These go as follows: 320 ppm for the spin-up run, 345 ppm for the historical run, 400 ppm for the near-term run, and 550 ppm for the long-term run.

Although other RCPs were available, due to time constraints, these were not addressed but will be considered in future work.

The satellite data integrated into TOPS come from numerous agencies (NASA, USGS, etc.), which in turn contain data necessary to calculate Leaf Area Index (LAI), Fraction of Photosynthetic Active Radiation (FPAR), and information about snow cover and melt[1]. More information on satellite derived data and processing can be found in R. Nemani et al. 2009, along with more specifics on the TOPS model.

Finally, the outputs we chose to work with from TOPS include GPP and soil moisture. VPD is a variable that is provided through CMIP5 models and calculated historically via PRISM data, thanks to the PRISM Climate Group from Oregon State University. These data were then plotted on maps via the Basemap module in Python.

b. Drought Modeling

For the Drought Code analysis, seven of the members of the CMIP5 project were used. Included were the BNU-ESM, CanESM2, CSIRO-Mk3.6.0, GFDL-ESM2G, GFDL-ESM2M, MIROC5, and MRI-CGCM3. These models were chosen because they were members of the NEX-DCP30 Downscaled 30 Arc-Second dataset and were stored in a format that we could efficiently aggregate to generate 30-year summaries[33]. The downscaling was performed on the following variables: precipitation rate, maximum temperature, and minimum temperature. The primary variable, Drought Code, is not a direct indicator of wildfire danger, rather it captures the state of deeper organic layers, those that take extended periods of time to properly dry. Crucially for this study, its calculation requires only maximum temperature, previous day's precipitation, and previous day's Drought Code, variables available in the downscaled dataset.

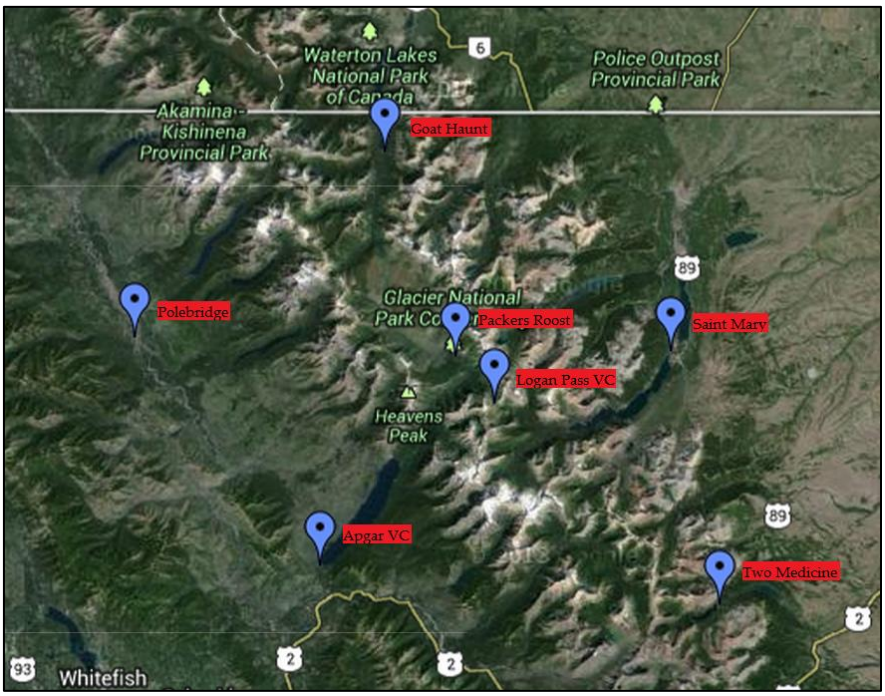

Figure 2. Locations in Glacier National Park Selected for Point Analysis

As Drought Code is generally computed on a daily basis, and because the downscaled data were stored in the form of monthly means, another step was necessary to obtain the daily estimates for maximum and minimum temperature, as well as precipitation rate. To do this, we chose domains enclosing one grid square from each model. From this box, for each day, we calculated the average values from the four corner grid points. With the high resolution data, we computed the anomaly for each 30 arc-second grid point within this domain for the month corresponding with the low-resolution day. In the case of precipitation, these anomalies were standardized against the monthly mean, while for temperature they were simply subtracted from the monthly mean. We then multiplied the daily precipitation values with the monthly precipitation anomalies and subtracted the temperature anomalies from the daily max/min temperature. This gave a reasonable representation of the daily conditions as calculated by each climate model at a much higher resolution than the model itself was able to compute. With these daily downscaled values, the other hurdle to overcome involved the estimation of the length of the winter season. Drought Code computation is not initiated until a region's "winter" has ended, which is operationally viewed as a location having a period of greater than 6C average temperatures for 3 consecutive days. For the purpose of this study, an estimate had to be made as to when "winter" began as well. Running some test cases, this was assessed to be a period of 5 consecutive days with average temperatures below 6C, which generally captured, if not the true start of winter, at least the time when fire danger was likely decreasing.

In order to accurately represent winter precipitation, which plays a role in the calculation of the initial Drought Code value once a location has thawed, estimates were made as to a conversion from millimeters of precipitation as output in the climate model to snowfall. This was performed by assuming a snow ratio of 1 mm snow-water-equivalent to 10 mm of pseudo-snowfall. For any location having a maximum temperature below 0C on a given day, all precipitation that fell at that location was assumed to be snowfall. Conversely, if a location with snow "on the ground" had a maximum temperature greater than 0C, the difference between that maximum temperature and 0C was subtracted (in centimeters) from the amount of snow, to simulate melting processes. This algorithm was tested in both Northern Utah and Central Wisconsin with realistic results for snowfall totals/distributions and timing of accumulation and melting. Locations with greater than 10 cm of snow on the ground were viewed to still be in winter, and Drought Code was not calculated.

Once Drought Code had been calculated for the domain, the monthly mean values for the following intervals were computed: 1970-1999, 2006-2035, 2036-2065, and 2066-2095. These were aggregated for the seven CMIP5 models used and ensemble mean, median, and standard deviation values were computed. Because the domains of each model run were not uniform, with the largest covering 2.5˚x2.5˚ and the smallest only 1˚x1˚, an assessment was made of the number of ensemble members covering each grid point as well. All seven of the models were analyzed over the primary region of interest, and for all four of the reference time periods. The only exception is that due to data availability, MIROC5 was not analyzed for the 2006-2035 period. Trend charts were generated containing all of the models along with the ensemble mean and median for a set of seven sites in Glacier National Park (Fig. 2). These locations were chosen from the National Park Service official map to represent a diverse set of elevations and climates.

c. Fire Behavior Modeling

A wildfire event in Glacier National Park was simulated using the Weather Research and Forecasting (WRF) model with the SFIRE physics extension. The technical equations and computational architecture underpinning WRF and SFIRE are described in great detail by Michalakes et al[24], Coen et al[22], Mandel et al.[23], among many others. Briefly, WRF is a highly advanced mesoscale climate model capable of simulating weather patterns in a three-dimensional environment using a series of nested vertical and horizontal grids. Weather processes are sequentially interpolated and downscaled to increasingly smaller, higher resolution domains situated within the original coarse layer. The smallest horizontal layer—the only one to directly interact with surface wind flow over local topography—forms the basis for an even finer-resolution subgrid that is the surface operated on by the fire model. Fire propagation is modeled using the Osher and Fedikew's[34] "level set method", allowing for greater flexibility over the tracer-based CAWFE fire model developed by NCAR. The two-dimensional fire spread model adapts equations developed by Roethermal[20] to a three-dimensional topographic environment influenced by surface-level winds calculated from the WRF model. As the fire spreads across the mesh subgrid, the model calculates the relative fraction of the fuel burned in each cell. Fuel properties per subgrid cell are input as fuel categories following Anderson[35]. At every time-step, the model interpolates wind at a height of 6.1 meters, influencing fire spread via the level-set function. The resulting heat flux from the fire is averaged across the cells that compose a single higher-order atmospheric cell, providing an iterative feedback between the fire and atmospheric models.

Wildland fire was modeled in the greater Glacier National Park region using data downloaded from the LANDFIRE and USGS National Map datasets, in addition to static world-wide data provided internally as a package for the WRF model. We built WRF/SFIRE on NASA Ames Research Center's *Pleiades* supercomputer using an online distribution (WRF version 3.3 with Sfire) provided by the Open Wildfire Modeling eCommunity (http://www.openwfm.org/wiki/Main_Page). WRF was compiled using a distributed memory (DMPAR) scheme using NETCDF "large-file" support to enable files larger than two gigabytes, which were expected given the large domain size. The WRF Preprocessing Suite (WPS), is a utility bundled with the main WRF distribution that enables relatively easy data processing from raw geotiff and NETCDF files to the geographic extent used by the WRF model. We interpolated the raw data (including high-resolution DEM and fuel data) to a region consisting of four nested domains (see Fig. 3) at 9000m., 3000m., 600m., and 120m. resolution. Our largest domain contained the entirety of the study region (roughly 550 by 490 km.), and the smallest region—where the fire submesh would operate—was bounded at 48 km^2. All of the domains were run using 41 vertical domains to appropriately simulate the multi-scaled atmospheric processes necessary for WRF. Weather data was extracted to the time frame of the model run, and interpolated to the physical domain using the attached Ungrib and Metgrid applications.

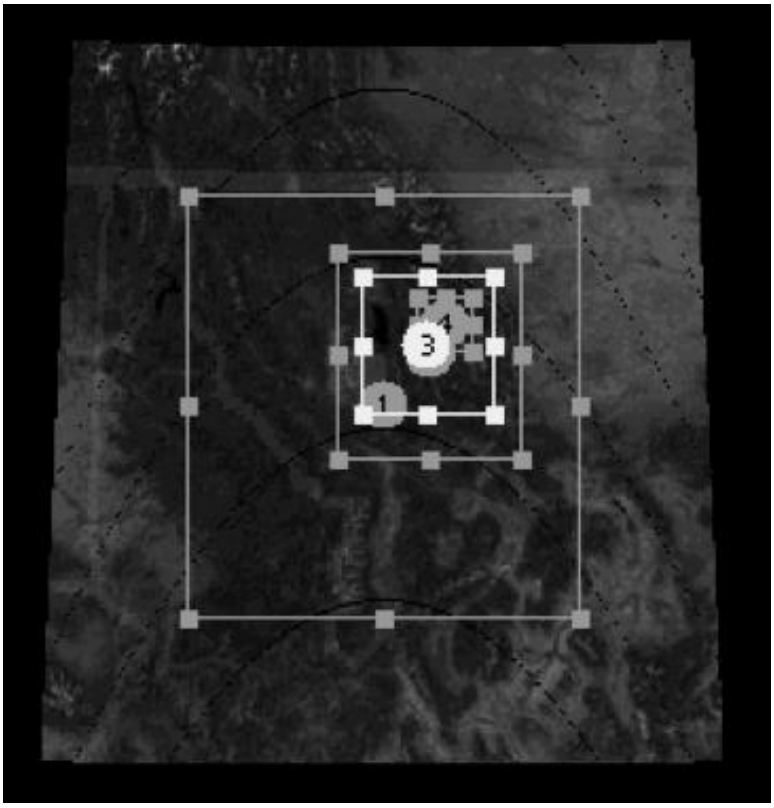

Figure 3. Map of four nested WRF/SFIRE domains. *Geogrid interpolates static 30 Arc-second data and high-resolution (30 m.) fuel and elevation data to each of the four domains above, at resolution of 9000m., 3000m., 600m., and 120m. respectively for each increasingly small domain. The final domain is the only one operated on by the fire mesh. The ignition point was chosen at the center of the smallest domain. Map data adapted from NCAR's Domain Wizard java runtime application.*

Following the preprocessing steps, WRF/SFIRE was run on the *Pleiades* supercomputer using six Westmere nodes for a total of 96 processors. The simulation modeled six hours of time across the domain on 1 JULY 2013, from 12:00:00 to 16:00:00 (UTC-6:00), with the fire ignition occurring as a 2-cell radius point at the rough center of the smallest domain five minutes into the simulation time. We used a short time step of 0.25 seconds to avoid issues with CFL condition error, as a larger time step would be insufficient to capture wind velocity occurring through the smallest fire submesh cells. We ran WRF/SFIRE using default parameters, except for eliminating cloud physics calculations and boundary-layer parameterization at the two highest-resolution domains to prevent excessive boundary layer error due to the extremely high-resolution WRF was being run at. The resulting WRF output files were converted in Python to VTK format. We visualized the model output as frames at thirty minutes and one hour using MayaVi to demonstrate the procession of fire over time, with streamlines used to represent higher-domain atmospheric wind and arrows indicating surface wind direction. Work is ongoing to complete an animated visualization for porting into Google Maps.

III. Results and Discussion

a. Ecological Modeling

Three map plots were created for each variable (GPP, VPD, and soil moisture), representing each time period, but subtracted from the near-term and long-term to get an idea of the differences between these. The month of August was chosen for these simulations in order to capture maximum snowmelt.

In Figure 4, difference values for GPP are plotted for: 1970-1999 vs. 2006-2035, 2006-2035 vs. 2066-2095, and 1970-1999 vs. 2066-2095 (as is for Figure 5 and 6). Although somewhat difficult to tell due to the resolution of

the model, displayed on the plots are the North Fork Flathead River (in black), which resides in a valley, with mountains on both sides. Lake McDonald is close to the south-center part of the plot, but is more easily seen in Figure 6, where values of soil moisture are recorded as zero (as they should). Analyzing these plots, it's evident that GPP drops in the valley, especially along the North Fork Flathead River, while increasing some along the slopes (and tops) of the mountains. These increases in GPP in the mountainous regions appear to occur more so between the historical and near-term scenarios, while leveling off in the plot of near-term vs. far-term. This could suggest an initial increase in ecosystem productivity in the mountains, and a decrease in ecosystem productivity for the historical and near-term runs. In the long-term run however, there is evidence that supports that the ecosystems that exist in the valley continue to be less productive, while ecosystems in the mountains produce little to no additional productivity. This makes sense in that; once we encounter a warmer climate inside Glacier National Park, various ecosystems will begin responding to changes in temperature, precipitation, and other variables associated with climate change. Although GPP is not by any means the only measure of ecosystem productivity, it does give insight on how the Greater Glacier National Park area could change in the 21st century.

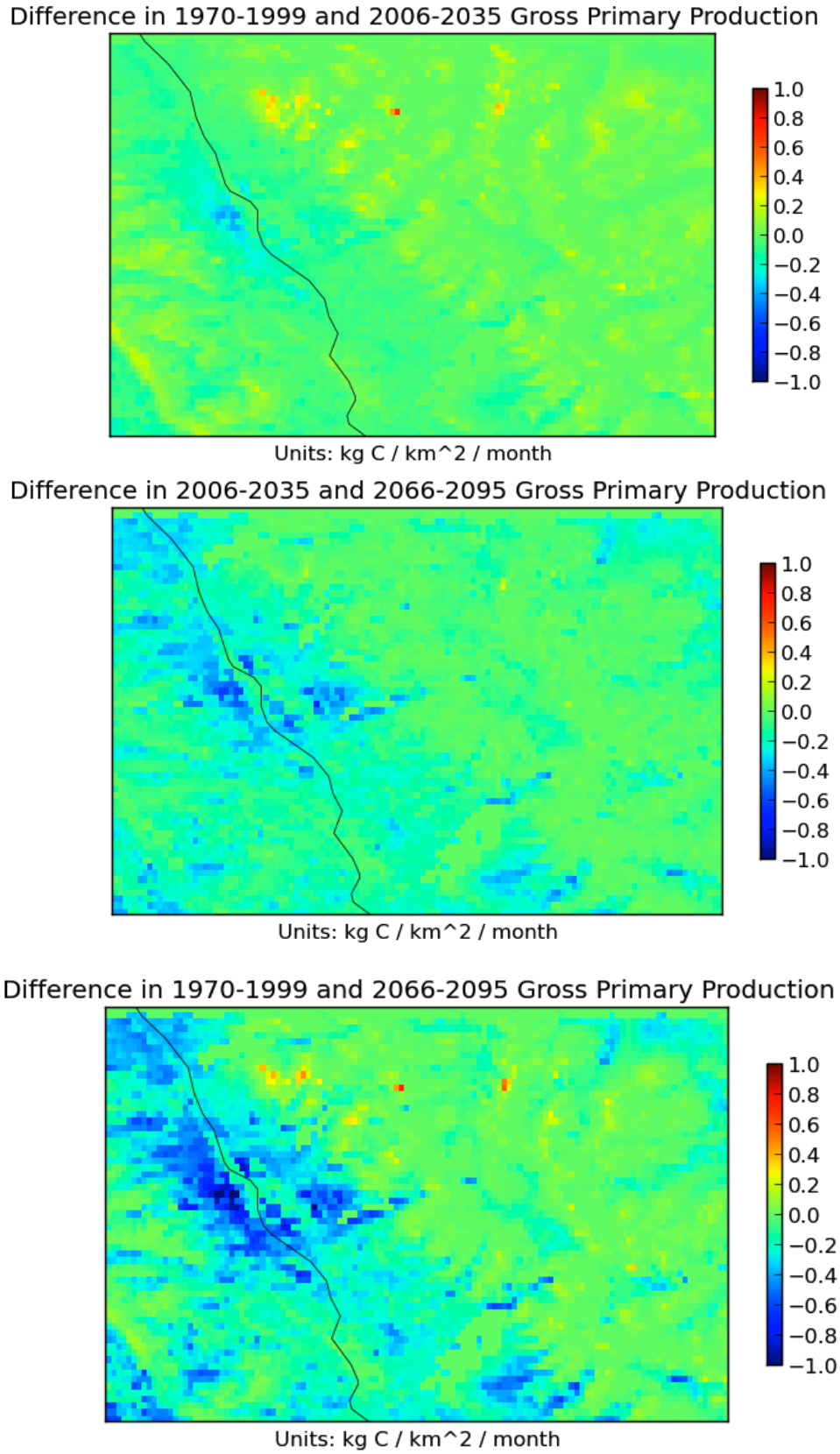

Figure 4. GPP difference plots of the three time periods.

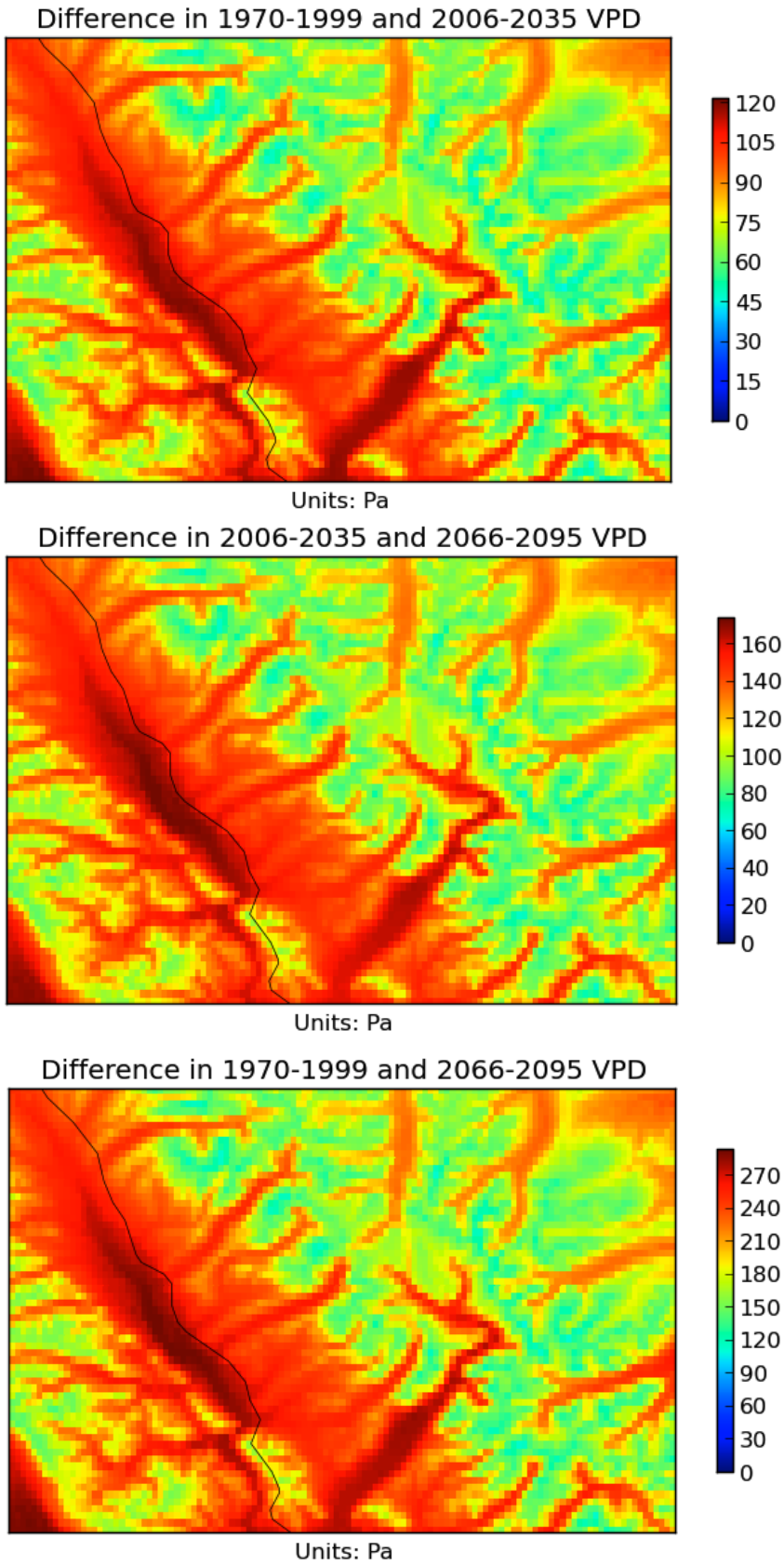

Figure 5. VPD difference plots of the three time periods.

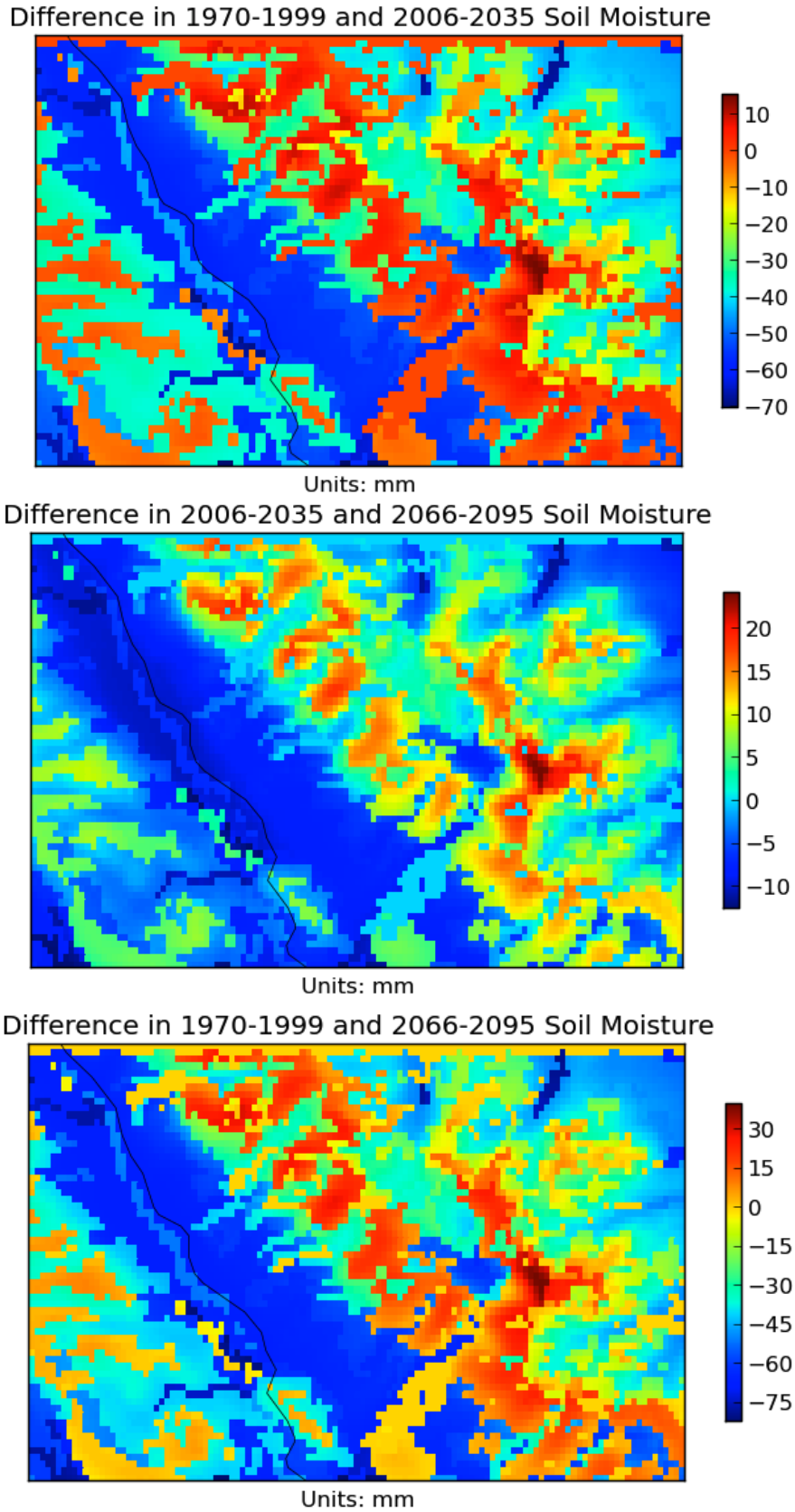

Figure 6. Soil moisture difference plots of the three time periods.

In Figure 5, difference values for VPD are plotted for the same time periods as in Figure 4. VPD, measured in Pascals, can be related to the amount of evapotranspiration that occurs in an ecosystem, with higher values corresponding to less evapotranspiration (since VPD is a difference in water vapor pressure and saturation water vapor pressure). These plots occur at a higher resolution (800 meter) since it is output from downscaled CMIP5 data, and not TOPS itself. From these plots, it's more evident where certain terrain occurs, such as the valley and flows of glacier/snow melt from the mountains. Although all of the subplots look fairly similar, the color bar values suggest that VPD is increasing throughout the Greater Glacier National Park area. In turn, this could indicate that less evapotranspiration is occurring in the park, leading to less productive and stressed vegetation and ecosystems.

In Figure 4, difference values for soil moisture are plotted. These images tell a slightly different story, in which all scenarios experience drier soils in the valley, with wetter soils in the mountains. This possibly implies that due to increased glacier/snow melt during the month of August, although some regions in the higher terrain areas see decreases in soil moisture as well, possibly hinting that no additional snowmelt is obtainable. Losses in soil moisture can put stress on current ecosystems in the park, and could help promote the advancement of wildfires.

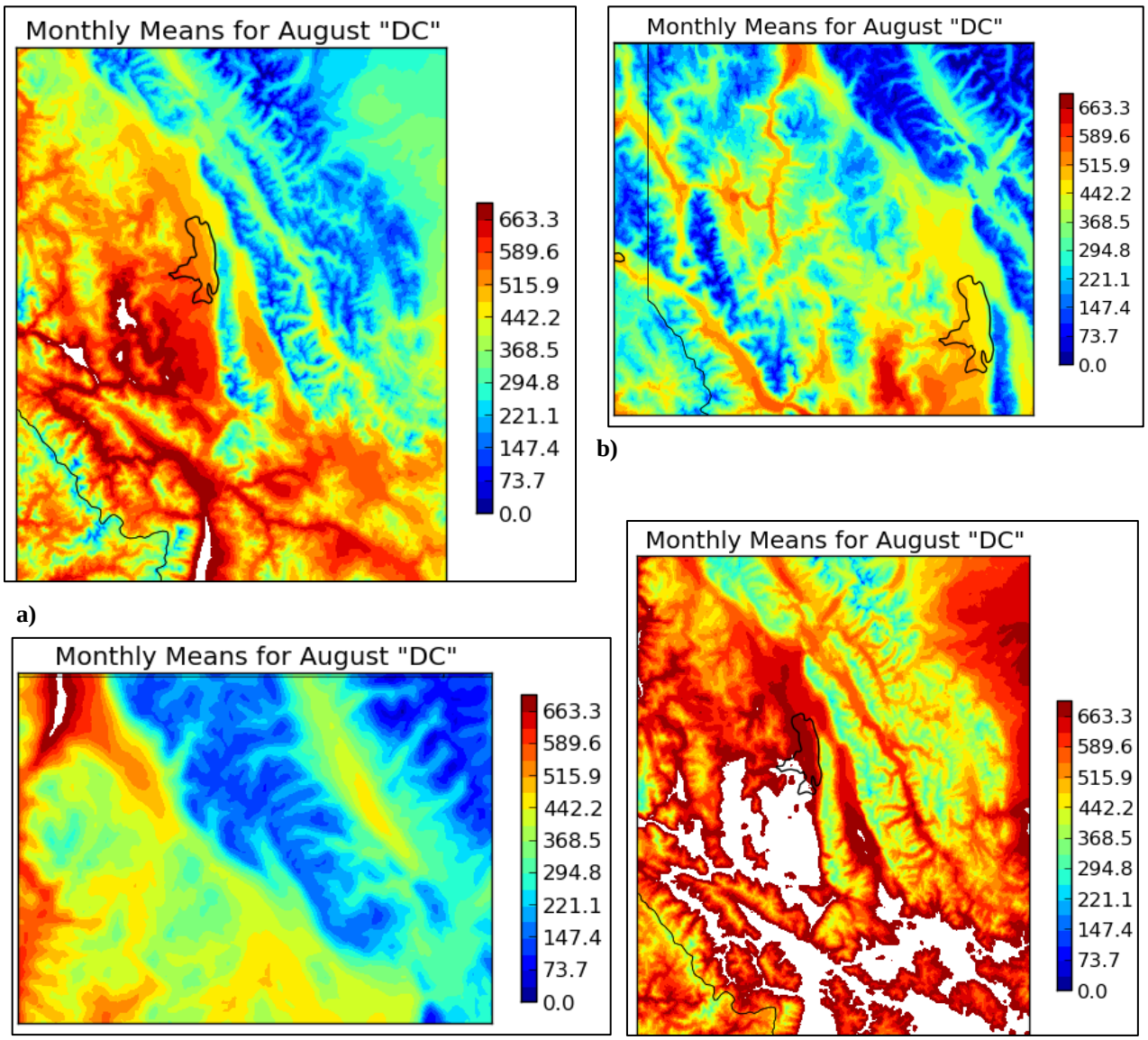

Figure 7a-d: August Monthly Mean Drought Code Values, 1970-1999, all values are unitless, a) BNU-ESM, b) GFDL-ESM2M, c) MIROC5, and d) CanESM2. All except for c) contain Flathead Lake as a reference point, while the domain of c) is north and west of the lake.

b. Drought Modeling

What appeared in the analysis output was that the different models, despite being initialized with the same radiative forcing, came to a very diverse set of conclusions as to projected values of Drought Code. For each of the selected images, the corners of the domain correspond to gridpoints in that model's grid, and the lake plotted in the majority of the images is Flathead Lake, which will be used as a reference given the different domains of the model analyses. For the historical period, 1970-1999 (Fig. 7a-d), the model reanalyses diverge quite dramatically. Values in the Kootenai River valley west of Glacier vary from around 500 in the BNU-ESM model to over 700 in the MIROC5. The interior valleys of the park range from close to 300 to over 500, and the mid-elevations from 200 to over 400. Again, note that these are from the historical runs, for which the models have been tuned to run closely with observations, yet there remains a significant difference between the run with the overall highest Drought Code values (CanESM2) and the lowest (GFDL-ESM2M). Sensitivity analysis is necessary to ascertain whether these disparities are due to higher temperatures, decreased precipitation, earlier spring thaw, or some combination.

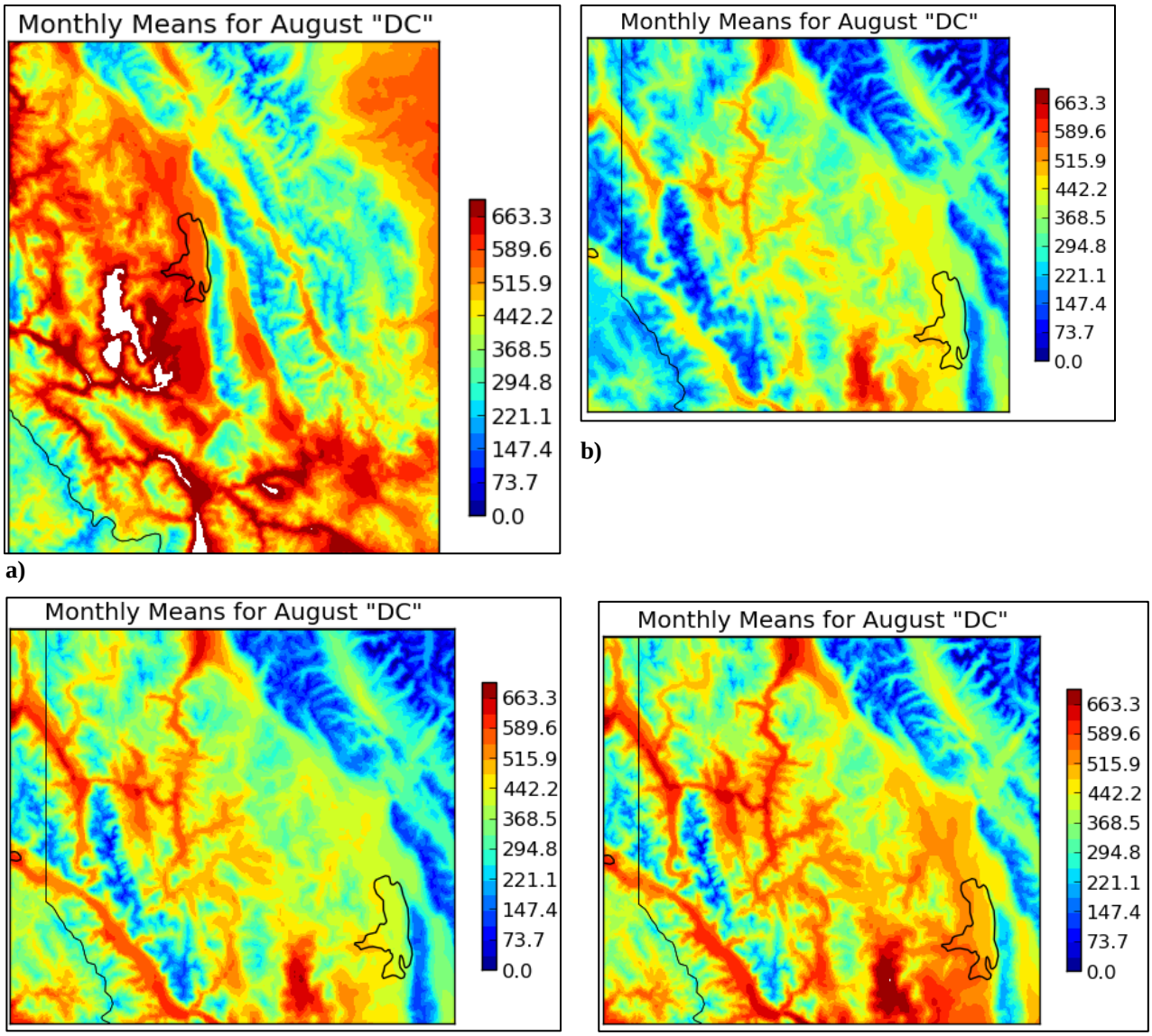

Figure 8a-d: August Monthly Mean Drought Code Values, 2066-2095, all values are unitless, a) BNU-ESM, b) CSIRO-Mk3.6.0 c) GFDL-ESM2M, and d) GFDL-ESM2G. All contain Flathead Lake as a reference point.

In Figure 8a-d, we look ahead to the far future projections, comprising the thirty year period from 2066 to 2095. Shown are three of the models with relatively low future projections (8b-d) and one, BNU-ESM, that shows a significant increase from the historical values to the far future. Again we see ranges in most locations greater than 200, perhaps most significantly in the mid-elevations. One of the primary advantages of the higher resolution dataset is its ability to resolve complex terrain features that would typically be broadened and flattened in a coarse climate model. This makes the analysis more useful in the Western United States as it gives management officials a better sense of specific drainages and canyons prone to accelerated impacts. As shown in the BNU-ESM simulation, Drought Code values of 300-400 will become common in August in forested regions that in the historical period averaged closer to 200. This suggests heavier organic fuels like downed trees will be more susceptible to wildland fire if these projections prove valid.

In Figure 10a-d, we show a single model, the MRI-CGCM3, as it projects September mean drought code values for each of the four time periods. Because Drought Code takes time to "spin up" from the initial values given following the previous winter, June and July have generally lower values regardless of their warmth or lack of precipitation, while August is the most consistently high-valued month throughout the region. September, however, can be the worst month at lower elevations, while temperatures at higher elevations begin dropping to the point that they return to "winter" conditions. Again, the key regions to watch are the mid-elevation mountain valleys and canyons. Under RCP 4.5 projections, the MRI-CGCM3 shows peak September mean monthly drought code values near Flathead Lake occurring during the 2036-2065 "middle-future" period, with values exceeding 600. However, values in the interior valleys of Glacier National Park increase from each 30 year span to the next, peaking above 300 during the 2066-2095 interval. Of note is that this level of discrimination is not possible in the coarser climate models, and only with statistical downscaling can we resolve these specific impacts.

By aggregating the Drought Code calculations from all seven of the models, we generated a series of ensemble images displaying the mean (Fig 11a-d) and standard deviation (Fig 9a-b) for the monthly means in each period. Note that the scale has changed to accommodate a wider range of values, as some of the values shown here are significantly higher than those shown in the MRI-CGCM3-only plots. This reflects the inclusion of wamer/drier models such as the CanESM2 (shown in Fig. 7a) and the BNU-ESM (Figs. 7b and 8a).What is not different about the ensemble is the extent of increase over the 125 year period, which is generally around 200 for most regions, including the mountain valleys of the park and many of the surrounding plains. Average Drought Codes above 400 are not prevalent inside the park boundaries in the historical ensemble in September, but by the 2066-2095 period, values this high are seen well into the higher reaches of the park, while valleys are averaging closer to 600.

Looking at the standard deviations, we find unsurprisingly that the historical values are significantly less than those from the 2066-2095 period. This initially diminishes the impact of the ensemble mean findings, as the spread indicated by the high standard deviations allows for, if we assert that the increase in Drought Code is around 200 for most of the terrain, not only no increase from the historical period to the end of the century, but also for decreased values. However, because Drought Code is not normally distributed but is bounded to be no less than zero, we can dismiss much of this argument on the grounds that higher values of Drought Code invite higher standard deviations, while low values, especially those near zero, ensure low value for standard deviation. In fact, as we saw in Figure 5, there is quite a wide variety of solutions for even the historical monthly average values for Drought Code, suggesting the spread has more to do with the models and less to do with the possibility that Drought Code might decrease rather than increase.

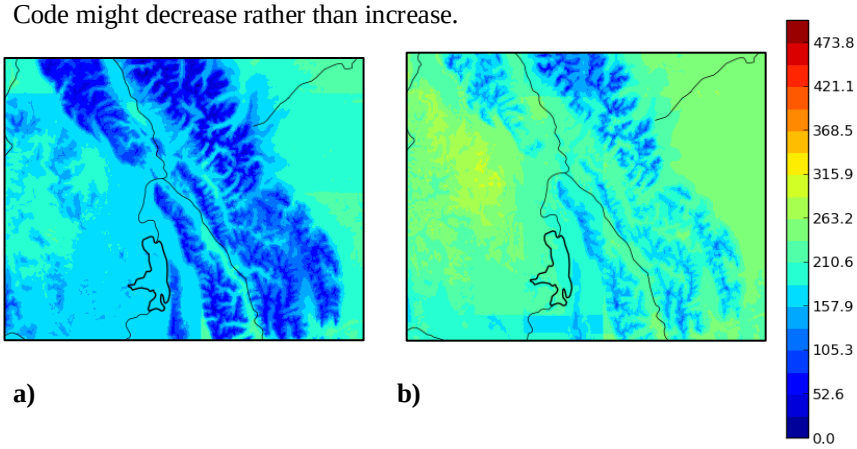

Figure 9a-b: Ensemble September Monthly Mean Standard Deviations for a) 1970-1999 and b) 2066-2095

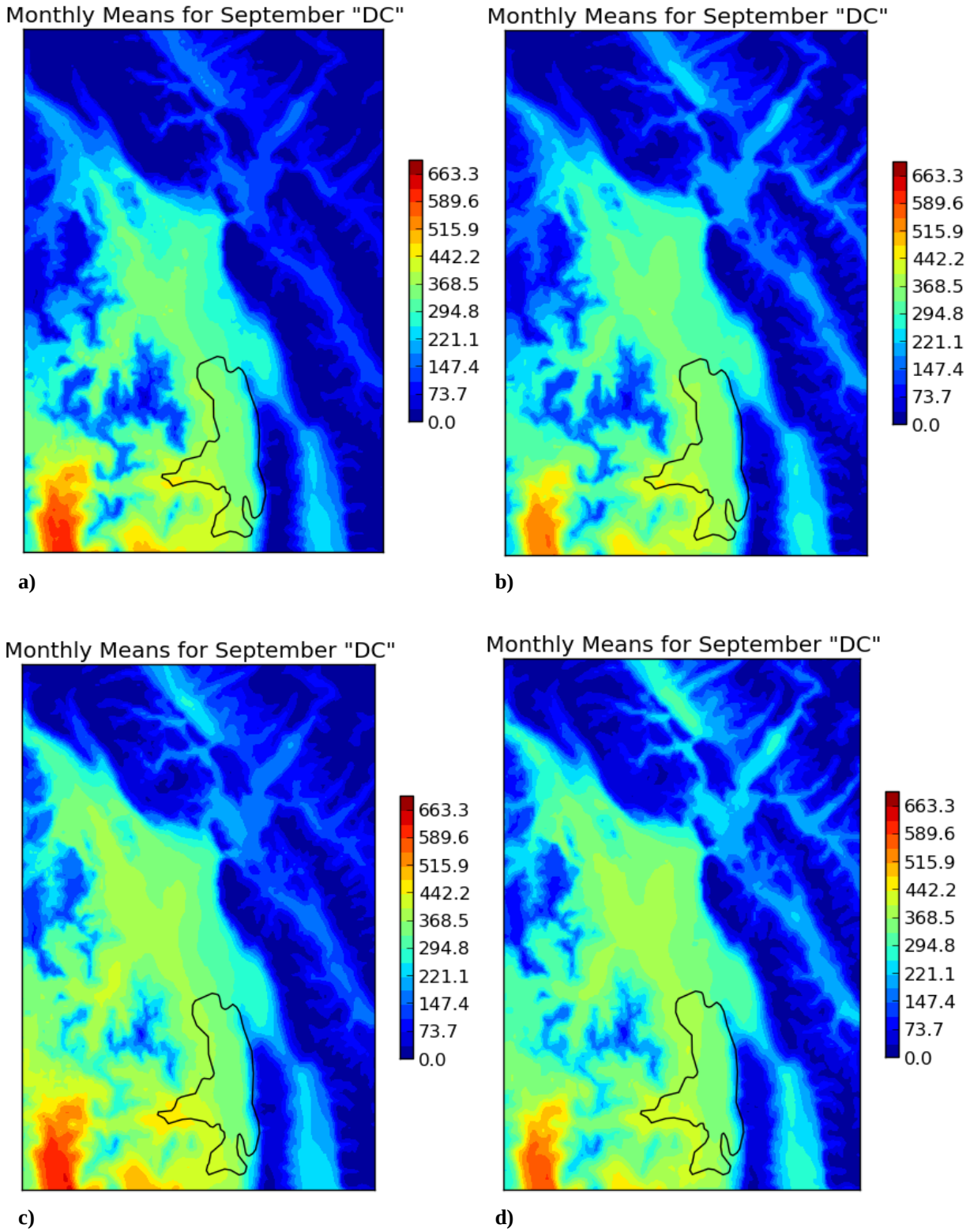

Figure 10a-d: September Monthly Mean Drought Code values from the MRI-CGCM3 model for the following time periods: a) 1970-1999, b) 2006-2035, c) 2036-2065, d) 2066-2095.

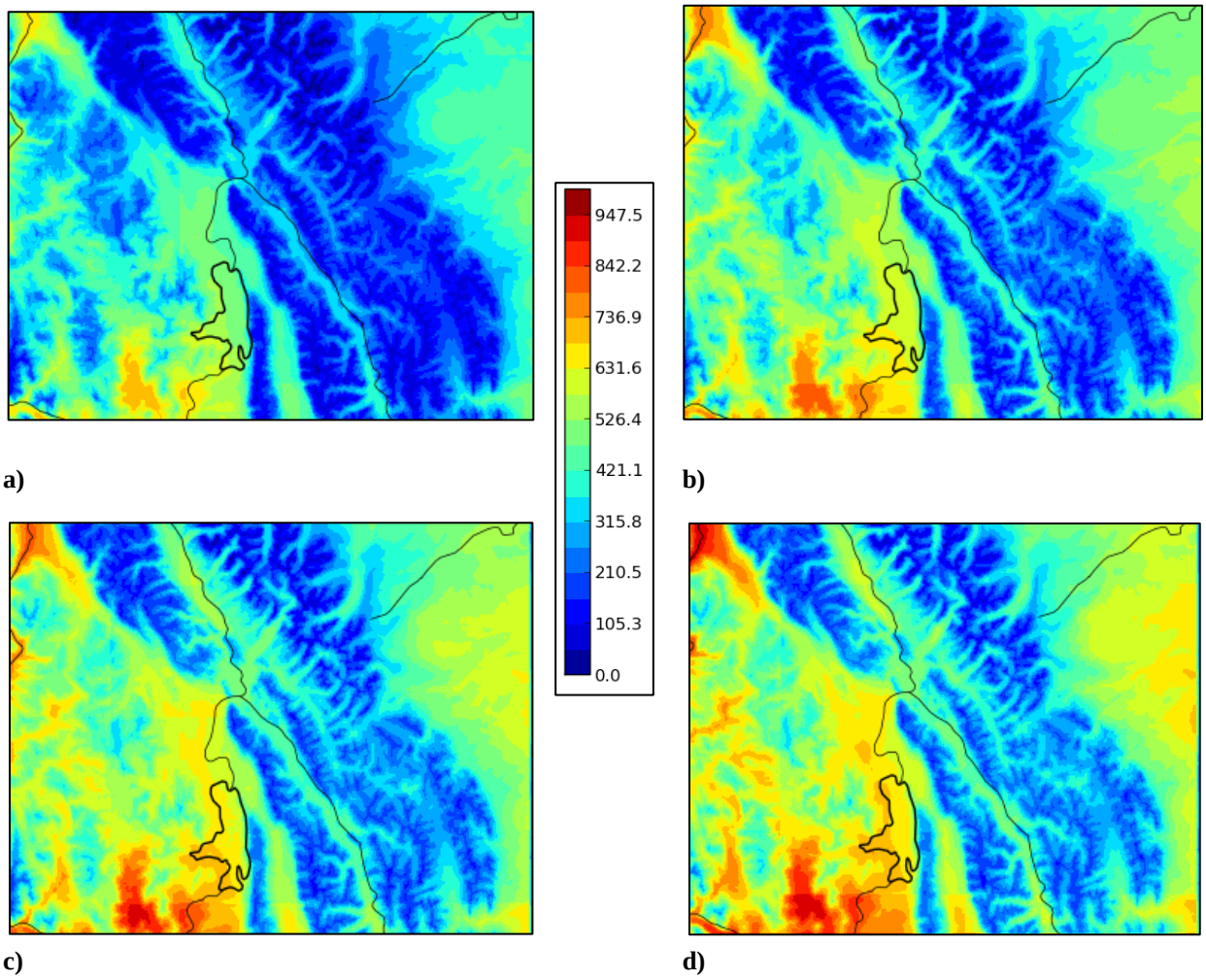

Figure 11a-d: Ensemble Means of September Monthly Means for the following time periods: a) 1970-1999, b) 2006-2035, c) 2036-2065, d) 2066-2095. Note the changed color scale for these figures (0-1000 versus 0-700) relative to previous figures.

This assertion is borne out by the trends at selected locations (Figure 12a-f). What these trend lines from the locations plotted in Figure 1 show is that though there is a fairly wide spread of solutions concerning Drought Code under RCP 4.5, the upward trend features in every one of them. The difference between each site, besides absolute location and elevation, is simply the magnitude of the Drought Code values. In every case, the ensemble mean (yellow line with diamond markers) increases by around 100. The outlier in terms of median value is Goat Haunt, where Drought Code appears to peak in the near-future with a significant drop off in the 2036-2065 period caused by decreases in three of the seven models. Also notable is the fact that in the two higher elevation sites, the MRI-CGCM3 and the two GFDL models appear to cluster close to zero, while the other four models show steady increases in Drought Code values. This suggests that perhaps the lower three models cool off too quickly in September, plunging these locations into "winter", while the other four do not exhibit this same issue.

As discussed previously, the CanESM2 has higher values at every location in every period, suggesting it is overly warm or dry relative to the other simulations. It is also the most aggressive at the two higher elevation locations in September, showing increases of nearly 300 at Packers Roost and 200 at Logan Pass. The models that appear to perform closest to the ensemble average are the MIROC5 and the BNU-ESM. In the three August plots,

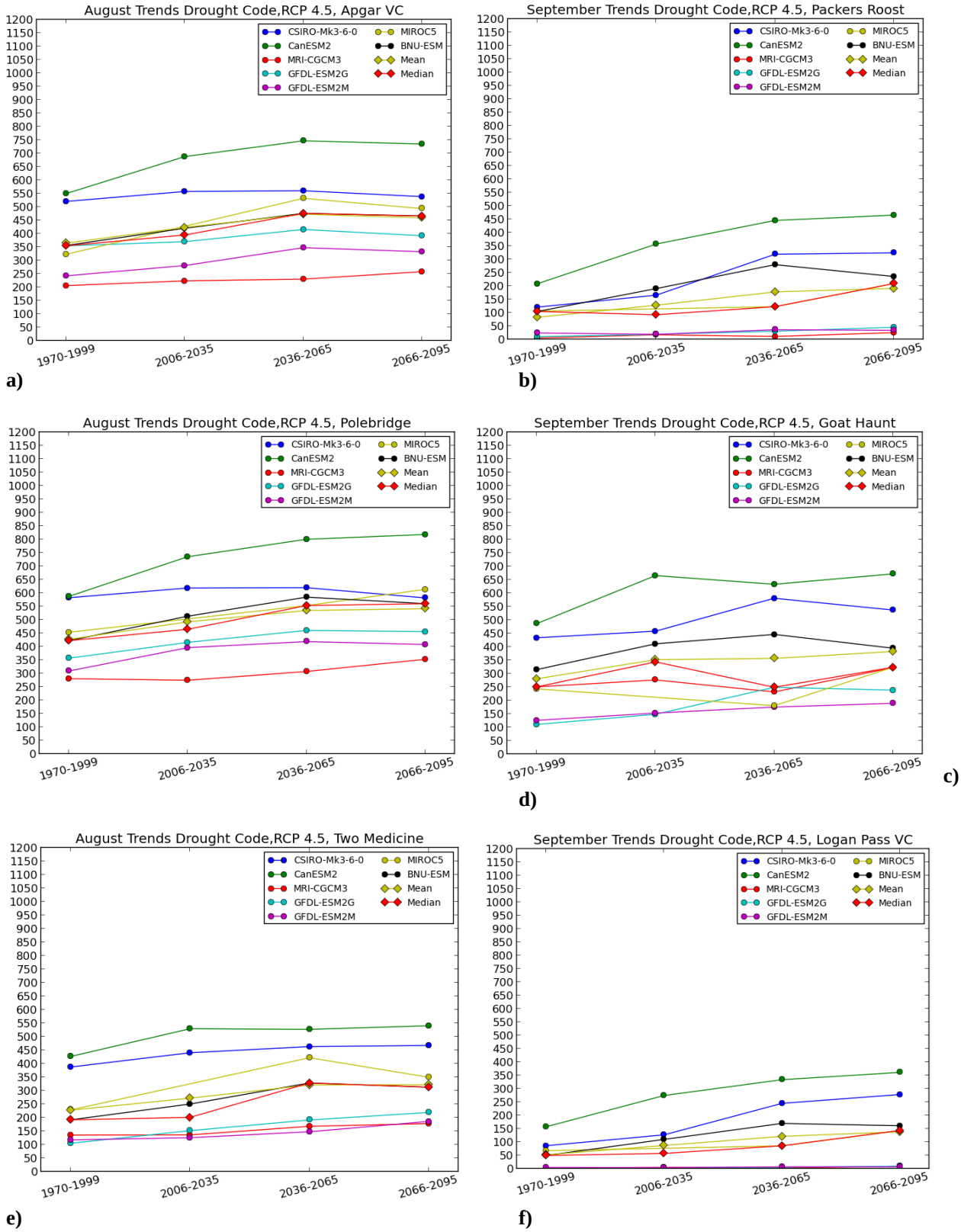

Figure 12a-f: Values for Monthly Mean Drought Code at six locations in Glacier National Park for all seven ensemble members as well as ensemble mean and median. Months and locations for each listed in titles.

each of which represents one of the mid-elevation locations, one interesting trend is that the highest ensemble average drought code values occur during the 2036-2065 period, leveling off or decreasing in the late-future. At Apgar Visitors Center and Two Medicine, this is for the most part driven by decreasing values in the MIROC5 model, while at Polebridge, both the CSIRO-Mk3.6.0 and BNU-ESM show declines from 2036-2065 to 2066-2095. Regardless, the important point to take away is that Drought Code values are increasing from historical averages at every location, in every model.

c. Fire Behavior Modeling

Fire modeling using the WRF/SFIRE setup demonstrates strong potential for use in research, despite significant barriers in terms of initial training and computational power. Initial WRF runs encountered significant error at larger time-steps, demonstrating the need for an extremely low number to avoid CFL condition error. WRF is, however, not built to run using an extremely high-resolution and short time-step conditions, generating boundary-layer errors at the furthest extent of the domain. The final run, consisting of a master domain of nearly 500 square kilometers, was still ongoing at the time of this writing. As such, visualization and modeling efforts are ongoing. WRF/SFIRE is currently successfully running in a high-performance computing architecture using a walltime of fourty hours and nearly 100 CPUs. The initial results for the simulation, however, suggest that the WRF/SFIRE simulation attempt require additional resources and time: WRF has not, at the time of writing, created a single restart file (slated to be generated every ten minutes in the simulation) despite a runtime of nearly twenty hours.

IV. Conclusion

The goal of the ecological modeling part of this study was to understand the basic functions of the Greater Glacier National Park area at the ecosystem level. The changes suggested to occur can help scientists and decision-makers better prepare for a changing park dynamic. Decreasing values of GPP, increasing values of VPD, and decreasing values of soil moisture in the main valley of the park can further enhance the likelihood of wildfires of starting and spreading further than previously possible. We acknowledge that the three variables used in this study do not ultimately describe the complex nature of the various ecosystems and terrain within the park, but it provides insight into how management practices of these lands can be honed to keep the park in the condition that was originally intended when first founded.

Glacier National Park has often been brought forward in the climate change discussion as a location that stands to lose a great deal as global temperatures increase. The park's namesake glaciers are receding at a rate suggesting they may no longer exist by mid-century. Our research suggests that losing these majestic masses of ice may not be the only significant impact to the park. The projected increases in August and September values of Drought Code throughout the region indicate that large organic fuels will be more susceptible to burning, leading to more sizeable and explosive wildland fires in and around the park. These fires, like the ones last year and this year in Colorado, have to potential to jeopardize park infrastructure and the tourism-driven regional economy. The mid-elevation glacial valleys and thriving forests of Glacier are most at risk as they will feel the first impacts of longer summers and increased potential for drought.

Two future extensions of this research include incorporating more models and radiative forcing scenarios, and expanding the dataset to allow for the calculation of more robust fire danger indices. Several more CMIP5 models have been downscaled to the 30 arc-second resolution, and analyzing their projections will increase the robustness of our findings. It is important to note that the results presented above focused on the RCP 4.5 climate change forcing, which assumes a moderate mitigation of current greenhouse gas emissions. However, data suggest that global emissions fall more in line with the RCP 8.5 scenario, which will have a more drastic impact on areas such as Glacier National Park. Analyzing less optimistic projections will give us a better idea of the extent to which we can expect indices such as Drought Code to elevate, as well as the locations in which the most intense increases will occur. Finally, Drought Code is only one of several intertwined fire danger metrics incorporated into the CFFDRS package. With downscaled wind speed and relative humidity projections, the entire suite of indices will be available, allowing us to get a better handle on the behavior of finer fuels, as well as occurrence of extreme fire danger.

Future research efforts are required to apply the WRF methodology on the scale necessary for landscape analysis. While WRF was successfully run at a relatively large 42 km^2 fire domain, a larger size is required for fire simulation across entire regions prone to fire. The process of running WRF mandates a significant deal of effort and training as well as access to large-scale computational resources, making the model impractical for use in operational fire-line environments. However, the model holds significant promise for developing a more nuanced and sophisticated understanding of the spatial location and likely behavior of fire in a future of higher temperatures

and drought. To assist in this regard, future effort is required to integrate both the ensemble-based CMIP-5 future weather and TOPS net primary productivity projections (converted to fire classes) for use in WRF/SFIRE. In addition to further visualization, integration of the output files to a GIS-based analysis would provide a more spatially robust analysis of fire spread, providing the ability for statistical The use of these inputs in a WRF/SFIRE simulation compared to a baseline current run would provide a useful understanding of how fire regimes would shift in the near and long-term future. The efforts and wildfire simulation presented here provide additional support for WRF/SFIRE as a useful tool for research purposes, allowing managers to provide more accurate fire-weather conditions in models than exist in most other operational software programs**.**

The more diverse the studies are on fire danger under current climate change estimates, the better prepared the fire community can be for managing and containing the fires that occur in the decades to come. With research like this and further advances in technology, we can more fully anticipate the challenges ahead when it comes to the protection of life and property from the threat of wildland fire.

References

[1]Nemani, Ramakrishna, et al. "Monitoring and forecasting ecosystem dynamics using the Terrestrial Observation and Prediction System (TOPS)." *Remote Sensing of Environment* 113.7 (2009): 1497-1509.

[2]Hashimoto, Hirofumi, et al. "Structural Uncertainty in Model-Simulated Trends of Global Gross Primary Production." *Remote Sensing* 5.3 (2013): 1258-1273.

[3]Churkina, G., S. W. Running, and A. L. Schloss. "Comparing global models of terrestrial net primary productivity (NPP): The importance of water availability."*Global Change Biology* 5.S1 (1999): 46-55.

[4]Krawchuk, M., Moritz, M., Parisien, M., Van Dorn, J., and Hayhoe, K.: Global Pyrogeography: the current and future distribution of wildfire, Plos One, **4**(4), 2009.

[5]Taylor, K.E., Stouffer, R.J., and Meehl, J.A.: An overview of CMIP5 and the experiment design, Bull. Am. Meteorol. Soc., **93**: 485-98, 2012.

[6]Moritz, M., Parisien, M., Batllori, E., Krawchuk, M., Van Dorn, J., Ganz, D., and Hayhoe, K.: Climate change and distruptions to global fire activity, Ecosphere, **3(6)**:49, 2012.

[7]Westerling, A.L., Bryant, B.P., Preisler, H.K., Holmes, T.P., Hidalgo, H.G., Das, T., and Shrestha, S.R.: Climate change and growth scenarios for California wildfire, Clim. Change, **109**: S445-S463, 2011.

[8]Litschert, S.E., Brown, T. C., and Theobald, D.M.: Historic and future wildfires in the Southern Rockies Ecoregion, USA, Forest Ecology and Management, **269:** 124-133, 2012.

[9]Spracklen, D.V, Mickley, L.J., Logan, J.A., Hudman, R.C., Yevich, R., Flannigan, M.D., and Westerling, A.L.: Impacts of climate change from 2000 to 2050 on wildfire activity and carbonaceous aerosol concentrations in the western United States, Journal of Geophysical Research, **114**:1-20, 2009.

[10]Westerling, A.L., Hidalgo, H.G., Cayan, D.R., and Swetnam, T.W.: Warming and earlier spring increase Western U.S. forest wildfire activity, Science, **313**: 940, 2006.

[11]Flannigan, M.D., and Van Wagner, C.E.: Climate change and wildfire in Canada, Can. J. For. Res. **21**: 66-72, 1991.

[12]Tymstra, C., Flannigan, M.D., Armitage, O.B., and Logan, K.: Impact of climate change on area burned in Alberta's boreal forest, International Journal of Wildland Fire, **16**: 153-160, 2007.

[13]Preisler, H. K., Chen, S., Fujioka, F., Benoit, J.W., and Westerling, A.L.: Wildland fire probabilities estimated from weather model-deduced monthly mean fire danger indices, International Journal of Wildland Fire, **17**: 305-316, 2008.

[14]Van Wagner, C.E.: Development and structure of the Canadian Forest Fire Weather Index system, Canadian Forestry Service Technical Report 35, Ottawa, 1987.

[15]Taylor, K.E., Stouffer, R.J., and Meehl, G.A.: A summary of the CMIP5 experiment design, 2009.

[16]Scott L. Stephens, Jason J. Moghaddas, Carl Edminster, Carl E. Fiedler, Sally Haase, Michael Harrington, Jon E. Keeley, Eric E. Knapp, James D. McIver, Kerry Metlen, Carl N. Skinner, and Andrew Youngblood 2009. Fire treatment effects on vegetation structure, fuels, and potential fire severity in western U.S. forests. Ecological Applications 19:305–320

[17] Barret, Stephen, Arno, Stepheh; Key, Carl. (1991). Fire regimes of western larch-lodgepole pine forests in Glacier National Park, Montana. Canadian Journal of Forest Research 21: 1711-1720.

[18] Finney, M. A.: FARSITE: Fire Area Simulator-model development and evaluation, Res. Pap. RMRS-RP-4, Ogden, UT: U.S. Department of Agriculture, Forest Service, Rocky Mountain Research Station, http://www.fs.fed.us/rm/pubs/rmrs rp004.html, 1998.

[19] Andrews, P. L.: BehavePlus fire modeling system: past, present, and future, Paper J2.1, 7th Symposium on Fire and Forest Meteorology, http://ams.confex.com/ams/pdfpapers/126669.pdf, 2007.

[20] Rothermel, R. C.: A Mathematical Model for Predicting Fire Spread in Wildland Fires, USDA Forest Service Research Paper INT-115, http://www.treesearch.fs.fed.us/pubs/32533, 1972.

[21] Coen, J. L.: Simulation of the Big Elk Fire using coupled atmosphere-fire modeling, International Journal of Wildland Fire, 14, 49–59, doi:10.1071/WF04047, 2005.

[22] Coen, J; Michalakes, J; Patton, E; Riggan, P; Yedinak, K. (2013). WRF-FIRE: Coupled Weather-Wildland Fire Modeling with the Weather Research and Forcasting Model. Journal of Applied Meteorological Climatology 52: 16-38.

[23] Mandel, Jan; Beezley, Jonathan; Kochanski, Adam. (2011). Coupled atmospheric -wildland fire modeling with WRF 3.3 and SFIRE 2011. Geoscientific Model Development 4: 591-610.

[24] Michalakes, J; Dudhia, J.; Gill, D.; Henderson, T; Klemp, J; Skamarock, W.; Wang, W. (2004). The Weather Research and Forecast Model: Software Architecture and Performance. Proceedings of the 11th ECMWF Workshop on the Use of High Performance Computing in Meteorology: 25-29.

[25] Kochanski, Adam, Kenkins, Mary Ann; Kruegar, Steven; Mandel, Jan; Beezley, Jonathan. (2013). Real time simulation of 2007 Santa Ana fires. Forest Ecology and Management 15: 136-149.

[26] Mika Peace, T. Mattner and G. Mills, The Kangaroo Island bushfires of 2007 A meteorological case study and WRF-fire simulation,Ninth Symposium on Fire and Forest Meteorology, Palm Springs, CA, October 18-20, 2011 (Adelaide University/Bureau of Meteorology, Adelaide, SA, Australia)

[27] Nina Dobrinkova, Georgi Jordanov, and Jan Mandel, WRF-Fire Applied in Bulgaria, Numerical Methods and Applications, I. Dimov, S. Dimova, and N. Kolkovska, eds., Lecture Notes in Computer Science 6046, Springer, Berlin/Heidelberg, 2011, pp. 133-140.

[28] Frederick L. Klasner and Daniel B. Fagre. Arctic, Antarctic, and Alpine Research, Vol. 34, No. 1 (Feb., 2002), pp. 49-56

[29]Keane, Robert E., Penelope Morgan, and Joseph D. White. "Temporal patterns of ecosystem processes on simulated landscapes in Glacier National Park, Montana, USA." *Landscape Ecology* 14.3 (1999): 311-329.

[30]Wang, Weile, et al. "Variations in atmospheric CO2 growth rates coupled with tropical temperature." *Proceedings of the National Academy of Sciences*(2013).

[31]Taylor, Karl E., Ronald J. Stouffer, and Gerald A. Meehl. "An overview of CMIP5 and the experiment design." *Bulletin of the American Meteorological Society* 93.4 (2012): 485-498.

[32]Thomson, Allison M., et al. "RCP4. 5: a pathway for stabilization of radiative forcing by 2100." *Climatic Change* 109.1-2 (2011): 77-94.

[33]Thrasher, B., Xiong, J., Wang, W., Melton, F., Michaelis, A., and Nemani, R.: New downscaled climate projections suitable for resource management in the U.S., Eos, Transactions American Geophysical Union (in review), 2013.

[34]S. Osher, R. Fedkiw, Level Set Methods and Dynamic Implicit Surfaces. Springer-Verlag New York, Applied Mathematical Sciences, 153, 2002

[35] Anderson, Hal E. 1982. Aids to determining fuel models for estimating fire behavior. USDA For. Serv. Gen. Tech. Rep. INT-122, 22p. lntermt. For. and Range Exp. Stn., Ogden, Utah 84401.